

Thermal stability of Cu and Fe nitrides and their applications for writing locally spin valves

C. Navío,¹ J. Alvarez,¹ M. J. Capitan,^{2,a)} J. Camarero,³ and R. Miranda^{1,3}

¹Dpto. de Física de la Materia Condensada, Universidad Autónoma de Madrid, 28049 Madrid, Spain

²Instituto de Estructura de la Materia, CSIC, c/Serrano 119, 28006 Madrid, Spain

³Instituto Madrileño de Estudios Avanzados en Nanociencia (IMDEA Nanociencia), Cantoblanco, Madrid, Spain and Dpto. de Física de la Materia Condensada, Universidad Autónoma de Madrid, 28049 Madrid, Spain

(Received 26 March 2009; accepted 5 June 2009; published online 2 July 2009)

We have studied the thermal stability of the Cu and Fe nitrides. These results show that a nanometer-thick Cu nitride film decomposes at the Fe₄N growth temperature. Considering this, we propose for their use in spintronics, the room temperature growth of a nonmagnetic (FeN)/semiconducting (Cu₃N) epitaxial nitride bilayer that transforms into a ferromagnetic (Fe₄N)/metallic (Cu) one by mild thermal annealing at 700 K. This process can be employed to locally decompose by laser (or ion) irradiation FeN/Cu₃N/Fe₄N trilayers, giving rise to an array of lithographically defined Fe₄N/Cu/Fe₄N spin valves surrounded by metal/semiconductor spacers. © 2009 American Institute of Physics. [DOI: 10.1063/1.3159630]

Spintronic devices are bound to dominate solid-state electronics in the near future, driven by scientific breakthroughs such as the giant magnetoresistance (GMR) (Ref. 1) or the tunnel magnetoresistance (TMR) effects, and their exceptionally rapid implementation in spin valves (SVs) and magnetic tunnel junction² products. Currently there is a strong drive to nanofabricate arrays of SVs or tunnel junctions for nonvolatile magnetic random access memories³ and related applications. The fabrication methods chosen mostly rely on cumbersome lithographic approaches to yield devices arranged with square symmetries, but there are applications in which simpler fabrication approaches might be required.

Cu₃N is a semiconducting material that is attracting increasing interest as a candidate to be used in spintronics applications. However, the thermal stability of Cu₃N is not well-known. Some authors^{4,5} have reported a decomposition temperature between 570 and 720 K for thick Cu₃N films, but others have found indications of decomposition at temperatures as low as ≈470 K.⁶ We have settled this issue in founding the temperature stability ranges for this compound in the thin film coverage range useful for the spintronics applications. Using a combination of spectroscopic and structural techniques, we have determined that at 700 K, Cu₃N films transform into Cu and, simultaneously, FeN into Fe₄N. From these results we propose here the basic steps for a thermal procedure to create SVs consisting of magnetic (Fe₄N)/metallic(Cu)/magnetic(Fe₄N) nanometer-thick epitaxial films by mildly heating locally a predeposited FeN/Cu₃N/Fe₄N laterally extended trilayer. This process can be employed to locally decompose by laser (or ion) irradiation the original trilayers giving rise to an array of SVs surrounded (and isolated) by metal/semiconductor spacers. This is demonstrated by studying separately under ultrahigh vacuum (UHV) conditions the growth and thermal decomposition of Cu₃N(100) films grown on Fe(100) and FeN(100) films grown on Cu(100), which are accurate model systems of the different components of the starting trilayers.

Figure 1 shows schematically the geometric arrangement and the type of materials used for the application proposed. FeN is a nonmagnetic metal with a low density of states (DOS) at the Fermi level and a zincblende structure that can be grown epitaxially on Cu(100).⁷ Cu₃N is a semiconductor with a cubic crystalline structure, a 1.25–1.8 eV band gap and a lattice parameter (3.815 Å) close to that of Fe₄N (3.795 Å), which can be grown epitaxially on Fe₄N(001) (Ref. 8) and Fe(001).⁹ Cubic γ'-Fe₄N (Ref. 10) is a low-resistance, oxidation resistant, high-magnetization material that can be grown epitaxially on different substrates.^{11–14} The bulk Curie temperature is 767 K and the saturation magnetization 1.8 T.

These all-nitride trilayers can be prepared simply by alternate evaporation of the different metals in a flux of highly reactive N atoms. Uniform, laterally homogeneous, epitaxial Cu₃N(001) films down to a thickness of 1.2 nm were grown at 300 K in an UHV chamber with a base pressure of 3 × 10⁻¹⁰ mbar by molecular-beam epitaxy of Cu in the presence of a beam of atomic nitrogen produced by a radio frequency (rf) plasma discharge source.¹⁵ Nitrogen was used as source gas in the rf plasma source with an internal pressure of 10⁻² mbar.⁹ The efficiency in the production of atomic N is 15% in the experimental conditions used. The iron nitride films were grown by codepositing Fe at a rate of 0.2 ML/min with a flux of atomic nitrogen. In this case, the rf source employed a 1:1 mixture of nitrogen and hydrogen. The sub-

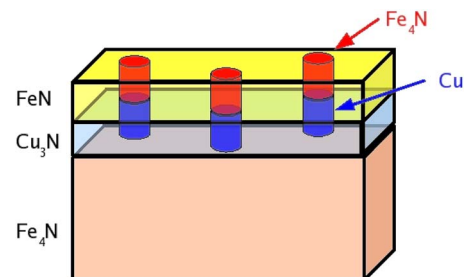


FIG. 1. (Color online) Schematic of an all-nitride FeN/Cu₃N/γ-Fe₄N trilayer that can be thermally driven to transform locally into a SV structure consisting of γ-Fe₄N/Cu/γ-Fe₄N immersed in a paramagnetic metal/semiconducting surrounding.

^{a)}Electronic mail: capitan@iem.cfmac.csic.es.

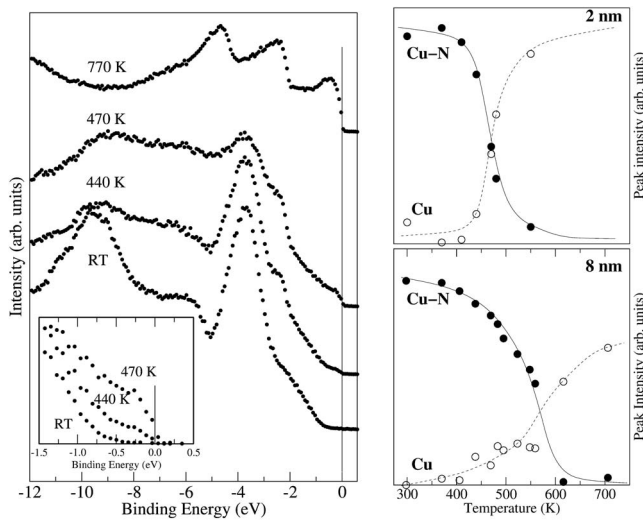


FIG. 2. Left panel: evolution of the UPS spectrum of a 5 nm thick $\text{Cu}_3\text{N}(001)$ film with increasing annealing temperatures. The film was grown on $\text{Fe}(100)$ and the spectra have been recorded with photons of 21.2 eV. The inset shows the DOS at the Fermi level. Right panels: evolution with annealing temperature of the area corresponding, respectively, to the Cu_3N (filled dots) and metallic Cu (empty dots) components of the Cu_{2p} XPS core level for Cu_3N films of two selected thicknesses (2 and 8 nm).

strate was kept at a temperature of either 665 or 300 K for the growth of γ' - Fe_4N and FeN , respectively. The chemical characterization, stoichiometry, and thickness of the grown films were determined *in situ* by x-ray photoelectron spectroscopy (XPS) ($h\nu=1253.6$ eV), while the DOS of the valence band was measured with ultraviolet photoelectron spectroscopy (UPS) using 21.2 eV photons. The magnetic characterization was performed *ex situ* at 300 K by means of high-resolution vectorial Kerr magnetometry measurements.¹⁶

In order to identify experimentally during the thermal treatments the composition of the different compounds and the specific bonding of N, we have studied the thermal stability of two model systems. First, we have studied the decomposition of Cu_3N films on $\text{Fe}(100)$ upon annealing. Since Cu_3N is a semiconductor, its transformation in metallic Cu can be followed with exquisite sensitivity by observing the appearance of metallic character, i.e., a finite DOS at the Fermi level. The left panel of Fig. 2 shows the evolution of the UPS spectra for a 5 nm thick $\text{Cu}_3\text{N}(001)$ film grown on $\text{Fe}(100)$ at increasing annealing temperatures. The initial Cu/N atomic ratio of the film was determined to be 2.8 ± 0.3 by quantitative XPS.¹⁷ The curve at the bottom of the figure shows the DOS of the film as-grown at 300 K, displaying a main peak at -3.8 eV and features at -6 and -9.5 eV related to the Cu_3N valence band, as indicated by first-principles calculations.⁹ Notice that there are no states at the Fermi level and the valence band edge is located at 0.65 eV below the Fermi level.

The inset in Fig. 2 shows that electronic states at the Fermi level can be first detected at 440 K, becoming clearly noticeable at 470 K. This signals a change from semiconducting character into metallic. The shoulder at -2.5 eV, which corresponds to the $3d$ band of metallic Cu, appears already at 440 K and increases at 470 K. At 700 K, the $\text{Cu}_3\text{N}(001)$ film has completely decomposed into metallic Cu. At 770 K, even the d -band of the $\text{Fe}(100)$ substrate is clearly visible close to the Fermi energy. In addition, N at-

oms have been partially transferred to the $\text{Fe}(001)$ substrate as indicated by the peak at -5 eV that corresponds to the $2p$ level of N adsorbed on $\text{Fe}(001)$.¹³ Given the extremely short mean free path of electrons with this kinetic energy, this implies that Fe regions must now be exposed to the vacuum, i.e., the thermal decomposition of the Cu_3N film results in a morphological modification, probably, a clustering process of the Cu formed on the surface. Thus, 770 K is the maximum temperature of processing.

In order to quantify the decomposition of Cu_3N into metallic Cu, the recorded $\text{Cu}_{2p_{3/2}}$ core level spectra (not shown) were fitted with two components corresponding to metallic Cu and Cu_3N , located at 932.3 and 932.7 eV, respectively, and their respective areas plotted as a function of the annealing temperature. The right panels in Fig. 2 shows the temperature evolution for selected film thicknesses of 2 and 8 nm, covering the relevant range for SV spacers. The films start to decompose at the same temperature (440 K), but the complete decomposition increases slightly with the thickness from 465–475 to 580 K. For the chosen model system, the decomposition of Cu_3N results in N transfer to the $\text{Fe}(100)$ substrate (in addition to desorption) and the corresponding growth of a nonmagnetic iron nitride at the interface. This does not occur when the underlying substrate is a N-stable Fe_4N film.

These results show that at the Fe_4N growth temperature¹⁴ the Cu_3N nanometer-thick film decomposes making unfeasible a $\text{Fe}_4\text{N}/\text{Cu}_3\text{N}/\text{Fe}_4\text{N}$ trilayer growth, as was suggested in Ref. 11 for the all-nitride technological spintronic applications.

The second model system concerns the thermal transformation of FeN on $\text{Cu}(100)$. The FeN film was grown by molecular-beam epitaxy of Fe in the presence of a beam of atomic nitrogen at a substrate temperature of 300 K. Quantitative XPS analysis of the resulting film shows an Fe/N stoichiometry of 1.1 ± 0.2 . X-ray diffraction (XRD) identifies the zincblende crystalline structure of γ' - FeN . The low-energy electron diffraction (LEED) pattern [see inset in Fig. 3(b)] is also consistent with $\text{FeN}(100)$. The film is paramagnetic.

This nonmagnetic FeN layer transforms into ferromagnetic γ' - Fe_4N by annealing at 700 K, as reflected in the corresponding N $1s$ core levels, LEED patterns, and hysteresis loops shown in Fig. 3. The lower right panel of Fig. 3 reproduces the XPS N $1s$ core level for the FeN film as deposited, and shows that, after heating, the XPS N $1s$ peak decreases in intensity and shifts to the known position and lineshape reported for thick γ' - Fe_4N films.⁷ The stoichiometry determined by XPS shows an atomic Fe/N ratio of 4.0 ± 0.2 and the Fe_{2p} core level is similar to the reference γ' - Fe_4N . The corresponding LEED pattern [Fig. 3(c)] is identical to that of γ' - $\text{Fe}_4\text{N}(100)$ surface [Fig. 3(d)].

The magnetic behavior of the γ' - Fe_4N layer has been studied by means of high-resolution vectorial Kerr magnetometry measurements shown in the lower left panel of Fig. 3 for two different films thicknesses. The films are ferromagnetic at 300 K, with remanence values close to 100% and display in-plane magnetization. The thinnest film, i.e., 1.7 nm, presents smaller coercive field, smoother magnetization reversal transition, and its magnetic anisotropy does not show the fourfold crystal symmetry of thicker film.¹⁸ This points out that in the nanometer range, these nitride films

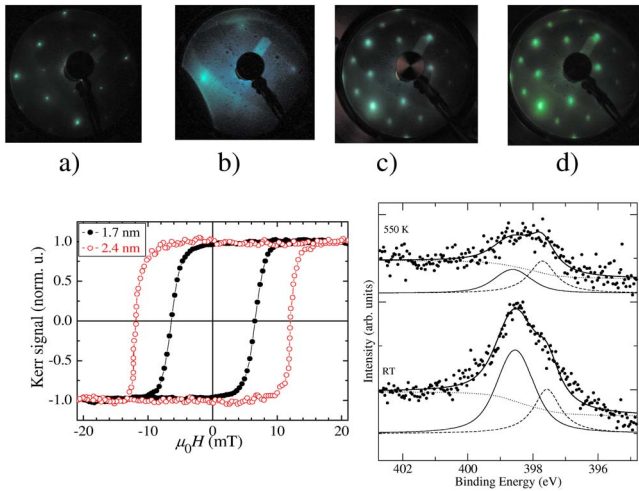


FIG. 3. (Color online) LEED patterns for (a) $c(2 \times 2)$ N on Fe(001), (b) a 32 Å thick FeN film on Cu(001) grown at 300 K, (c) this film after annealing at 715 K, and (d) reference γ' -Fe₄N(100) thin film. Notice that (c) and (d) are identical. Lower left panel: room temperature Kerr magnetization curves for 1.7 nm (filled circles) and 2.4 nm (empty circles) thick γ -Fe₄N films. Lower right panel: N 1s core level for the FeN film deposited at 300 K and after heating to 715 K. The last one is identical to the corresponding spectrum for a thick γ -Fe₄N(100) film.

present a thickness dependence of the Curie temperature, as generally found for low-dimensional ferromagnetic systems.^{19,20}

We stress that in the temperature range of transformation of nonmagnetic FeN into magnetic γ' -Fe₄N, Cu₃N decomposes into metallic Cu. Thus, a soft thermal treatment of an all-nitride FeN/Cu₃N/Fe₄N trilayer results in a (Fe₄N/Cu/Fe₄N) magnetic/metal/magnetic trilayer, with the required properties to act as a SV, with the further advantage that, by using a local heating probe, SVs can be directly written on an appropriate environment.

This work had financial support from both MICINN (Grant No. FIS 2007-61114, CONSOLIDER on Molecular

Nanoscience, Grant Nos. FP2001-1310 and MAT2004-05865), and CM (Nanomagnet program).

¹M. N. Baibich, J. M. Broto, A. Fert, F. Nguyen Van Dau, F. Petroff, P. Etienne, G. Creuzet, A. Friederich, and J. Chazelas, *Phys. Rev. Lett.* **61**, 2472 (1988).

²J. S. Moodera, L. R. Kinder, T. M. Wong, and R. Meservey, *Phys. Rev. Lett.* **74**, 3273 (1995).

³“Magnetic RAM Today,” Memory Strategies International (March 2007).

⁴M. Asano, K. Umeda, and A. Tasaki, *Jpn. J. Appl. Phys., Part 1* **29**, 1985 (1990).

⁵T. Nosaka, M. Yoshitake, A. Oakamoto, S. Ogawa, and Y. Nakayama, *Appl. Surf. Sci.* **169**, 358 (2001).

⁶Z. Q. Liu, W. J. Wang, S. Chao, and S. K. Zheng, *Thin Solid Films* **325**, 55 (1998).

⁷C. Navío, J. Álvarez, M. J. Capitán, F. Yndurain, and R. Miranda, *Phys. Rev. B* **78**, 155417 (2008).

⁸D. M. Borsa, S. Grachev, C. Presura, and D. O. Boerma, *Appl. Phys. Lett.* **80**, 1823 (2002).

⁹C. Navío, M. J. Capitán, J. Álvarez, F. Yndurain, and R. Miranda, *Phys. Rev. B* **76**, 085105 (2007).

¹⁰J. Q. Xiao and C. L. Chien, *Appl. Phys. Lett.* **64**, 384 (1994).

¹¹D. M. Borsa, S. Grachev, J. W. J. Kerssemakers, and D. O. Boerma, *Appl. Phys. Lett.* **79**, 994 (2001).

¹²J. M. Gallego, S. Y. Grachev, D. M. Borsa, D. O. Boerma, D. Ecija, and R. Miranda, *Phys. Rev. B* **70**, 115417 (2004).

¹³J. M. Gallego, D. O. Boerma, R. Miranda, and F. Yndurain, *Phys. Rev. Lett.* **95**, 136102 (2005).

¹⁴C. Navío, J. Álvarez, M. J. Capitán, D. Ecija, J. M. Gallego, F. Yndurain, and R. Miranda, *Phys. Rev. B* **75**, 125422 (2007).

¹⁵S. Grachev, D. M. Borsa, S. Vongtragool, and D. O. Boerma, *Surf. Sci.* **482**, 802 (2001).

¹⁶J. Camarero, J. Sort, A. Hoffmann, M. García-Martín, B. Dieny, R. Miranda, and J. Nogués, *Phys. Rev. Lett.* **95**, 057204 (2005).

¹⁷J. Alvarez, J. J. Hinarejos, E. G. Michel, J. M. Gallego, A. L. Vazquez de Parga, J. dela Figuera, C. Ocal, and R. Miranda, *Appl. Phys. Lett.* **59**, 99 (1991).

¹⁸D. Ecija, E. Jimenez, J. Camarero, J. M. Gallego, J. Vogel, N. Mikuszeit, N. Sacristan, and R. Miranda, *J. Magn. Magn. Mater.* **316**, 321 (2007).

¹⁹R. Miranda, F. Yndurain, D. Chandesris, J. Lecante, and Y. Petroff, *Phys. Rev. B* **25**, 527 (1982).

²⁰C. M. Schneider, P. Bressler, P. Schuster, J. Kirschner, J. J. de Miguel, and R. Miranda, *Phys. Rev. Lett.* **64**, 1059 (1990).